16,04

Photonic modes of dielectric Möbius resonator with one and two twists

© M.E. Bochkarev[1,2], N.S. Solodovchenko[1,2], K.B. Samusev[1,2], M.F. Limonov[1,2,¶]

[1] Ioffe Institute,
St. Petersburg, Russia
[2] ITMO University,
St. Petersburg, Russia
¶ E-mail: M.Limonov@mail.ioffe.ru

Received October 21, 2025
Revised October 21, 2025
Accepted October 24, 2025

In this study, three types of dielectric resonators were created and investigated: a flat ring resonator and Möbius resonators with one and two twists. The resonators have the same rectangular cross-section and midline length, as well as the same permittivity. The centimeter-sized resonators were created on a 3D printer, and the extinction spectra were experimentally studied in the microwave range in an anechoic chamber. The main result of the study is the experimental demonstration of a half-period shift of longitudinal photon modes in the scattering spectrum of a Möbius resonator with one twist relative to the spectra of a flat ring, which is associated with the appearance of the Berry phase π, and the absence of a shift in the spectra of a Möbius resonator with two twists due to an additional phase incursion of 2π, corresponding to the resonance condition for the longitudinal modes of a flat ring.

Keywords: Möbius resonator, ring resonator, Berry phase, longitudinal photonic modes.

DOI: 10.61011/PSS.2025.10.62649.284-25

1. Introduction

The classic Möbius strip is itself a one-sided surface formed by joining two ends of a sufficiently long rectangular strip of paper twisted into one or more half turns, called „twists“ [1,2]. In this article, we'll examine the dielectric Möbius strips of finite thickness twisted into one or two twists (i.e., one complete revolution), and we will call such an object a Möbius resonator (MR). MR has only two faces (two undirected Möbius strips), only two edges, and has no vertices. Unlike a one-sided Möbius strip with a one-sided topology, a MR of finite thickness with any number of revolutions is topologically identical to an ordinary ring resonator.

The significant interest of researchers in the Möbius strip is largely due to the optical properties associated with the so-called Berry phase, which determines the polarization state of an electromagnetic wave in optical fibers with a non-trivial shape. During propagation, the polarization of an electromagnetic wave is determined by two mechanisms, first, the usual dynamic phase shift associated with the passage of the optical path, and, secondly, an additional phase multiplier, which is independent of the length of the optical path, but has a geometric nature. This additional phase shift, first described by Pancharatnam in 1956 [3] and generalized by Berry in 1984 [4,5], is dubbed Pancharatnam−Berry phase, or simply Berry phase. It turned out that this exotic addition to the usual phase shift can be observed experimentally and studied theoretically in optics [6–8], acoustics [9], various solid-state systems [10,11], in cosmology [12].

Going back to the main topic of our article, we note that the relationship between the geometry and physical properties of nano- and microscopic structures of the Möbius strip has been already analyzed in the literature [1,13–17]. In particular, specific electronic states were observed that determine the aromaticity of Möbius [18] and the properties of twisted semiconductor tapes [19], abnormal plasmonic modes formed in metallic Möbius nanostructures [20], and the behavior of the Berry phase was experimentally studied at changing the thickness of the Möbius strip from flat rectangular to square [8].

In this paper, we experimentally and theoretically investigate the resonant optical properties of Möbius dielectric resonators with one and two twists in comparison with the properties of a flat dielectric ring of the same thickness, width, and length along the midline of the structures. The photonic properties of flat dielectric rings have previously been studied in detail in a number of papers [21–25]. In particular, in the scattering spectra of dielectric rings, we observed exceptional points of [23] and Fano resonances of [21,25], and found cascades of bound states in the continuum [24]. The nontrivial behavior of photonic resonances was observed during the transition from a closed dielectric ring to an open ring with a change in the resonator topology [26].

Based on detailed information about the photonic properties of flat dielectric rings, in this paper we interpreted the observed effects in the scattering spectra of Möbius dielectric resonators with one and two twists. As far as we know from the literature, the scattering spectra of a two-twist Möbius resonator have not been studied before.

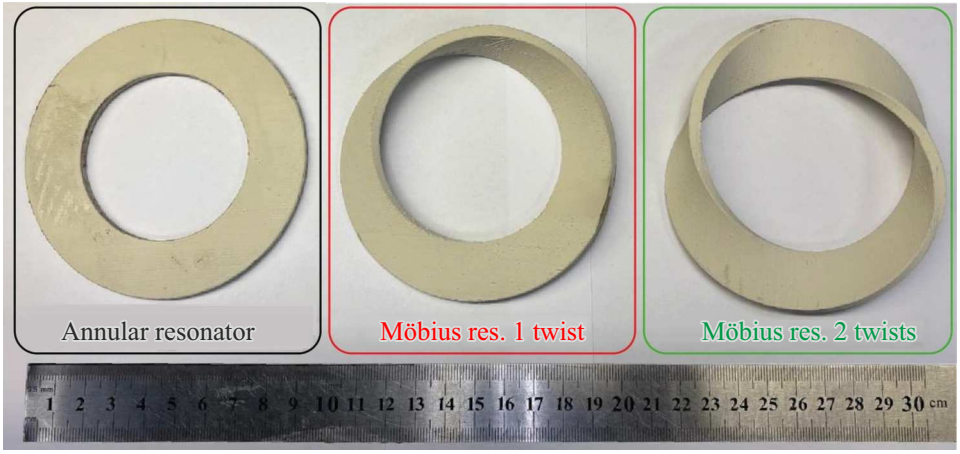

Figure 1. Photo of three experimental samples. On the left — a flat ring resonator, in the middle — Möbius resonator with one twist, on the right — Möbius resonator with two twists. A centimeter ruler is provided to illustrate the dimensions.

2. Method of analysis, samples fabrication and experimental studies

The purpose of this work is to study the transformation of photonic modes in a Möbius dielectric resonator with a change in the number of twists. As is known, Maxwell equations have the property of scalability for media without dispersion of permittivity ε and magnetic susceptibility μ, therefore our results are valid for any spectral range, both optical and microwave. Therefore, the extinction and scattering of electromagnetic waves by a particle of arbitrary shape is determined only by the ratio of its characteristic dimensions and the wavelength of the incident radiation, as well as the values of ε and μ at a given wavelength. The parameters of the samples studied in the work, typical of the optical range, were used as the dielectric constant, namely $\varepsilon = 8.23$ and material losses $\mathrm{tg}\,\delta = 1.1\,\mathrm{e}^{-3}$ [27]. The analysis results are presented depending on the dimensionless reduced frequency normalized to the characteristic size of the structure, defined as $x = 2R_{\mathrm{out}}/\lambda$, where λ is the incident wavelength, and R_{out} is the outer radius of the structure.

A plastic filament „ZetaMix epsilon 10 filament", which is an ABS matrix with a 80 % titanium dioxide content, was used to fabricate samples of the ring resonator and Möbius resonators with one and two twists. Printing was carried out in ITMO University (St. Petersburg) using a FlyingBear Reborn 2 3D printer, which is based on the principle of layer-by-layer creation of a three-dimensional object according to a given program. Since the fragility of the material due to high content of titanium dioxide, the plastic coil was suspended at a height of one meter above the 3D printer. Printing mode: nozzle temperature is about 280 °C, heating platform temperature is 110 °C. According to the recommendations of the plastic filament manufacturer [27], the application rate of the material for the first layer was 2.5 mm/s and 15 mm/s for subsequent layers. As a result, three resonators were printed: a ring resonator and two Möbius resonators with one and two twists, Figure 1, which took 6, 13 and 18 h to print, respectively. The increased printing time is explained by the need to print additional supporting structures with a more complex resonator geometry. All resonators have permanent cross-section. The geometry of the resonators was modeled by rotating a rectangular section with a width of $W = 20$ mm and a height of $h = 4$ mm along a circle with a radius of $R_{\mathrm{central}} = 40$ mm, which corresponds to the ratio of the inner radius to the outer $R_{\mathrm{in}}/R_{\mathrm{out}} = 0.6$. The dimensions were chosen so that the longitudinal modes of the resonators fall into the frequency range from 4 to 8 GHz, which corresponds to the parameter $2R_{\mathrm{out}}/\lambda$ from 1.40 to 2.56.

The selected frequency range made it possible to measure the extinction cross-section using optical theorem in an anechoic chamber at ITMO University [21,22] by method of micrometer microscopy. The measurements were carried out using a Russian-made dual-port vector network analyzer (Planar S5085), to which two horn antennas (TRIM 0.75–18 GHz) were connected, forming a quasi-plane wave installed at a distance of three meters from each other. The frequency range from 1 to 8.5 GHz was scanned using 16001 frequency point. Parameter S_{21} of the scattering matrix was measured twice: first in free space S_{21}^b, and then with a sample S_{21}^s placed between the antennas. According to the optical theorem, the imaginary part of the forward scattering amplitude is proportional to the effective scattering area. Thus, the extinction cross-section was calculated using the formula

$$\sigma_{\mathrm{ext}}(\omega) = \frac{4\pi}{k}\,\mathrm{Im}\left(\frac{S_{21}^s}{S_{21}^b}\right)L, \qquad (1)$$

where L is the distance from the sample to the receiving antenna, which was 1.5 m, and k is the wave vector of

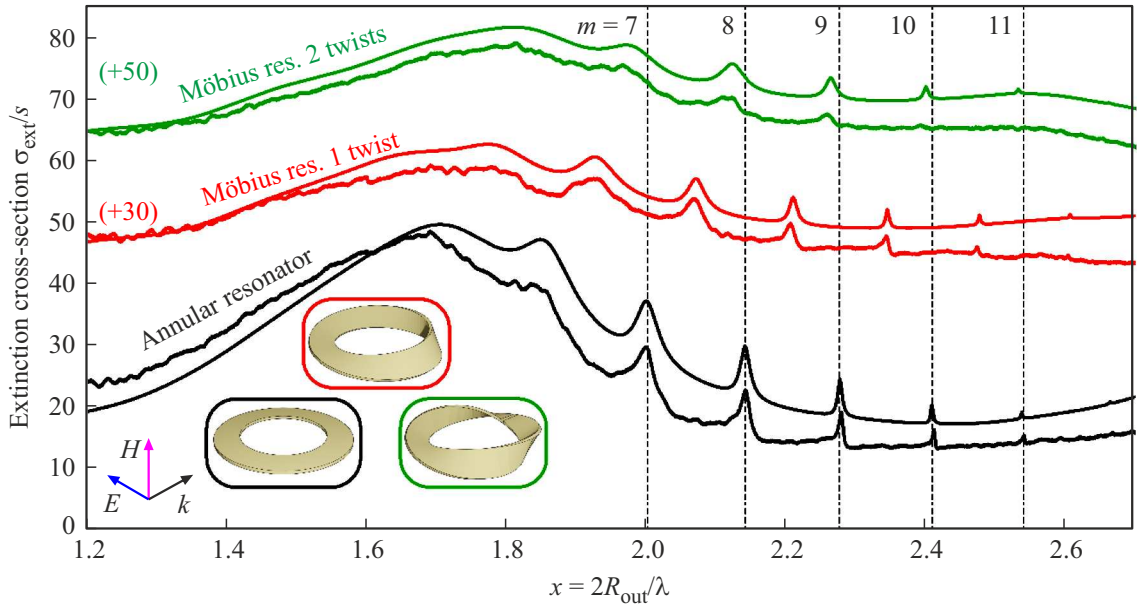

Figure 2. Experimental light scattering spectra (spectra with low noise) and calculated scattering spectra (smooth curves) for a flat ring resonator (black), Möbius resonator with one twist (red) and two twists (green) in the region of the first photon gallery ($r = 1$, $z = 0$). The photos of the samples are placed in frames that match the color of the scattering spectra. The spectra are shifted vertically by the specified values. The indexing of the longitudinal azimuthal modes of the flat ring $(1, 0, m)$ is shown at the top of the figure. Dimensionless frequency $x = 2R_{out}/\lambda$.

the incident wave. The values of the extinction cross-sections obtained both in calculations and in the experiment were normalized to the geometric shadow of the resonator, defined as $S = 2R_{out}/h$.

COMSOL Multiphysics program was used for analysis, which allows using an optical module to find eigen values (resonant frequencies) and eigen functions (electromagnetic field distributions), as well as calculate the extinction cross-section [24,25]. In three-dimensional flat ring resonators, the eigen functions can be conditionally characterized by an azimuthal (m) and two transverse mode indices along the width (r) and height (z) of the cross-section, forming an ordered triple (m, r, z). To calculate the eigen values and eigen functions „Natural frequency" mode was used in COMSOL, while the resonator was surrounded by a perfectly matched layer, and there was no incident wave. To calculate the extinction cross-section, the „Frequency domain" mode was used, in which the plane wave (the excitation geometry is shown by a triple of vectors **k**, **E**, **H** in Figure 2) changes at each frequency.

3. Results and discussion

The low-frequency photon spectrum of a flat dielectric ring with a rectangular cross-section differs significantly from the well-known spectrum of modes of the whispering gallery [28], related to dielectric resonators in the form of a disk. The modes of the whispering gallery arise inside the disk due to total internal reflections from the side wall when the phase condition is met after bypassing the entire resonator, whereas in an annular resonator, due to the presence of an inner wall, total internal reflection occurs on both surfaces [29,30]. Thus, the low-frequency photon spectrum of a dielectric ring with a rectangular cross-section consists of a number of galleries, each of which begins with a wide Fabry–Perot resonance between opposite walls: radial resonances of Fabry–Perot (index r) occur between a pair of side walls, axial resonances of Fabry–Perot (index z) occur between the upper and lower walls [21,22]. Each gallery continues with an equidistant sequence of longitudinal resonances (azimuth index m) with exponentially increasing Q-factor.

In this paper, we study three dielectric resonators (a flat ring and two Möbius strips), all with a rectangular cross-section whose width is greater than the height ($20 \times 4\,mm^2$). In this case, the first photon gallery begins with a Fabry-Perot resonance along the width with indexes ($r = 1$, $z = 0$), Figure 2 [21]. As can be seen from the figure, the Q-factor of the azimuthal resonances of the corresponding gallery increases exponentially at $m > 6$, while the lower modes form a wide low-frequency hump in the extinction spectrum [21]. For modes with an azimuth index $m > 11$, the radiation quality factor of the modes exceeds the material one, which is why the resonance intensity decreases, and the corresponding lines become indistinguishable neither in the experiment nor in numerical analysis.

Azimuthal indexes m are assigned to resonances based on the calculation of photonic modes (eigen vectors), Figure 3.

Of the greatest interest is the relative spectral position of the azimuthal modes in the spectra of the Möbius resonator

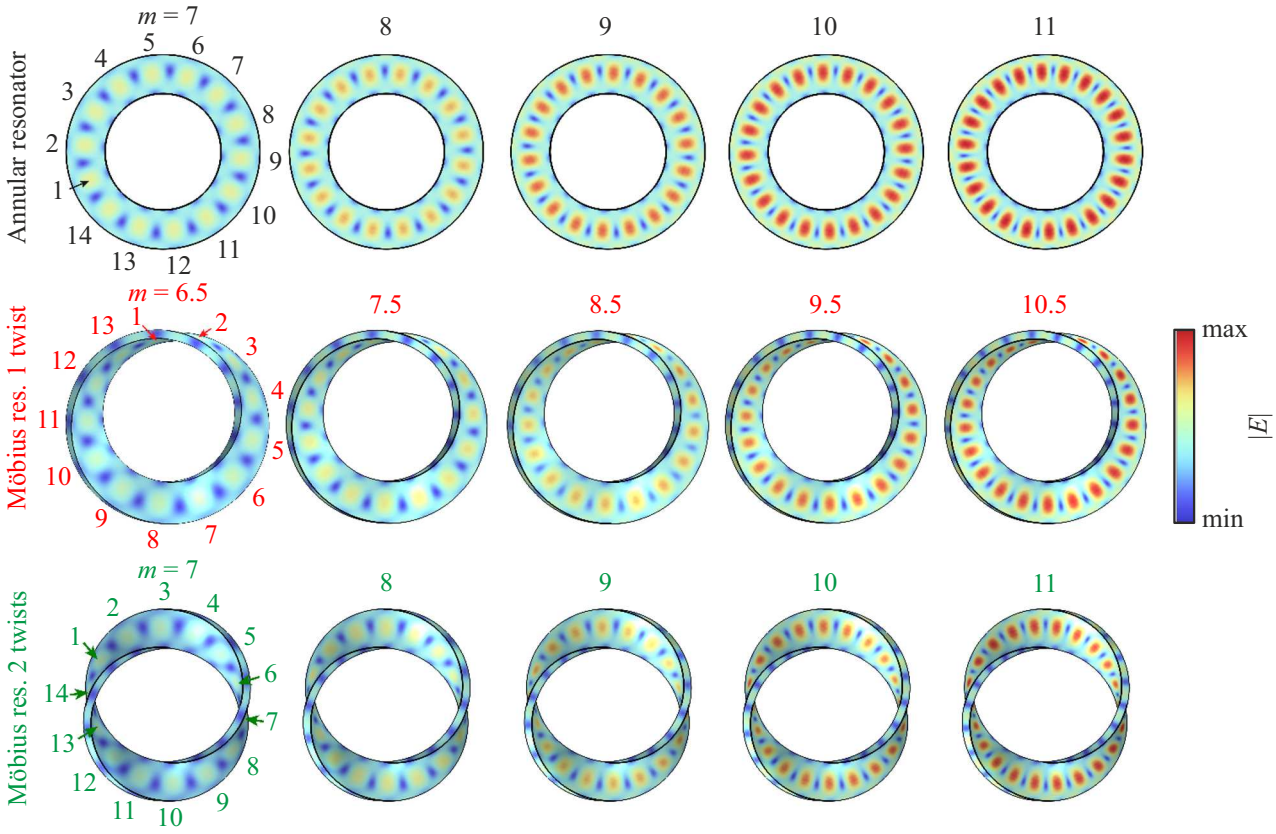

Figure 3. Electric field eigen mode modulus distributions for a flat ring resonator (top row), Möbius resonator with one twist (middle row) and two twists (bottom row) in the region of the first photon gallery.

with one and two twists relative to the modes of the flat ring. As can be seen from Figure 2, all the azimuthal 1-twist Möbius modes are shifted by exactly half a period relative to the equidistant sequence of azimuthal modes of the flat ring. This effect was experimentally observed earlier and is due to the Berry phase [3–5], the magnitude of which varies from 0 to π depending on the ratio of width and height in the cross section of a single-twist Möbius resonator [8]. Qualitatively, the explanation boils down to the following: in a thin (width $\gg$ height) resonator, when a linearly polarized wave propagates, the vector **E** is oriented strictly along the long wall and, when the resonator is twisted, rotates in space together with the resonator itself. In the case of a single twist, i. e., a rotation by 180°, after completing the entire path at the end, the vector **E** is also expanded by 180° relative to the initial orientation, which corresponds to an additional geometric phase π. This means that a mode that is resonant in a flat ring with a wavelength of $L_{\text{ring}} = m\lambda_{\text{Ring}}$ and is determined only by the dynamic phase shift along the ring $2\pi m$ will not be resonant in a Möbius resonator due to the additional geometric Berry phase π. Accordingly, the resonant modes in a thin Möbius resonator will be determined by the total dynamic and geometric phase condition $kL + \pi = 2\pi m$ (k — wavenumber), and all resonant frequencies will be shifted by half relative to the flat ring $L = \lambda(m - 1/2)$ [8].

The original experimental result of this work is a demonstration of the scattering spectrum of a 2-twist Möbius resonator (green spectra in Figure 2). Following the described algorithm, we conclude that the photon mode, which has an azimuthal index of m in a flat ring, changes the direction of the vector **E** twice to 180° in the process of completely bypassing the 2-twist Möbius resonator, that is, it comes to the beginning of the path in the phase. This effect corresponds to the geometric Berry phase 2π. Therefore, in Figure 2, the Möbius modes with two twists (green spectra) are close in frequency to the modes of the flat ring (black spectra). One of the reasons for the slight shift between the modes of the flat ring and the 2-twist Möbius modes is due to the low dielectric constant, which in turn affects the Q-factor of the resonances. Figure 2 illustrates that with an increase in the azimuth index m and, accordingly, an increase in the Q-factor of the mode [21], the frequency shift declines.

Note that the shape of the longitudinal mode line in the calculated spectra is close to the Lorentz contour, although in the general case of scattering extinction it reflects the interference of the Fan between the incident and scattered waves. As noted earlier [33], in some cases the resonant lines can practically coincide in contour shape with the Lorentz contour, corresponding to the case of the Fano resonance with the asymmetry parameter $q \to \infty$.

4. Conclusion

The Möbius resonator provides extensive possibilities for manipulating the behavior of various particles, such as electrons, polaritons, and photons. When an electromagnetic wave propagates in a flat ($R_{out} - R_{in} \gg h$) dielectric Möbius resonator, an additional geometric Berry phase appears, which is combined with the usual dynamic phase, depending only on the length of the resonator. As a result, with an odd number of twists, starting from one, the appearance of the Berry phase $N\pi$, where N is an odd integer, leads to a shift in the resonant conditions for a closed bypass by half a wavelength. It should be stressed that with an increase in N, there is no „accumulation" effect, i. e., for any odd N, the wavelength decreases only by half. At the same time, for any Möbius resonator with an even number of twists $2N$, the Berry phase equal to $2N\pi$ does not lead to a change in the resonant phase condition and the resonant wavelength remains unchanged.

It is interesting to draw an analogy with the photonic effects that are observed during another transition between two structures with different topologies, namely, between a dielectric planar ring and a planar split ring [26]. During this transition, each pair of doubly degenerate azimuthal ring modes (clockwise and counterclockwise propagation) splits into „ordinary" and „topological" modes. In „ordinary" modes, the azimuth index m does not change, while in topological modes it does, but unlike in the case of the Möbius resonator, it does not decrease, but increases by half $(m + 1/2)$.

Funding

The authors express their thanks for the grant support from RSF No. 23-12-00114.

Conflict of interest

The authors declare that they have no conflict of interest.

References

[1] S. Tanda, T. Tsuneta, Y. Okajima, K. Inagaki, K. Yamaya, N. Hatakenaka. Nature **417**, *6887*, 397 (2002).
[2] E.L. Starostin, G.H.M. Van der Heijden. Nature Mater. **6**, *8*, 563 (2007).
[3] S. Pancharatnam. Proc. Indian Acad. Sci. **44**, *5*, 247 (1956).
[4] M.V. Berry. Proceed. R. Soc. Lond. A **392**, *1802*, 45 (1984).
[5] M.V. Berry. Nature **326**, *6110*, 277 (1987).
[6] H.P. Breuer, K. Dietz, M. Holthaus. Phys. Rev. A **47**, *1*, 725 (1993).
[7] Y.Q. Cai, G. Papini, W.R. Wood, S.R. Valluri. Quantum Optics **1**, *1*, 49 (1989).
[8] J. Wang, S. Valligatla, Y. Yin, L. Schwarz, M. Medina-Sánchez, S. Baunack, C.H. Lee, R. Thomale, S. Li, V.M. Fomin, L. Ma, O.G. Schmidt. Nature Photon. **17**, *1*, 120 (2022).
[9] M. Xiao, G. Ma, Z. Yang, P. Sheng, Z.Q. Zhang, C.T. Chan. Nature Phys. **11**, *3*, 240 (2015).
[10] J. Wang, S.-C. Zhang. Nature Mater. **16**, *11*, 1062 (2017).
[11] Y. Zhang, Y.-W. Tan, H.L. Stormer, P. Kim. Nature **438**, *7065*, 201(2005).
[12] D.P. Datta. Phys. Rev. D **48**, *12*, 5746 (1993).
[13] S. Tanda, T. Tsuneta, T. Toshima, T. Matsuura, M. Tsubota. J. Physique IV **131**, 289 (2005).
[14] J. Gravesen, M. Willatzen. Phys. Rev. A **72**, *3*, 032108 (2005).
[15] Z. Li, L.R. Ram-Mohan. Phys. Rev. B **85**, *19*, 195438 (2012).
[16] N. Nishiguchi, M.N. Wybourne. J. Phys. Commun. **2**, *8*, 085002 (2018).
[17] S.O. Demokritov, A.A. Serga, V.E. Demidov, B. Hillebrands, M.P. Kostylev, B.A. Kalinikos. Nature **426**, *6963*, 159 (2003).
[18] H.S. Rzepa. Chem. Rev. **105**, *10*, 3697 (2005).
[19] V.M. Fomin, S. Kiravittaya, O.G. Schmidt. Phys. Rev. B **86**, *19*, 195421 (2012).
[20] Y. Yin, S. Li, V. Engemaier, E.S.G. Naz, S. Giudicatti, L. Ma, O.G. Schmidt. Laser Photon. Rev. **11**, *2*, 1600219 (2017).
[21] N. Solodovchenko, M. Sidorenko, T. Seidov, I. Popov, E. Nenasheva, K. Samusev, M. Limonov. Mater. Today **60**, 69 (2022).
[22] A.P. Chetverikova, M.F. Limonov, M.S. Sidorenko, K.B. Samusev, N.S. Solodovchenko. PNFA **57**, 101185 (2023).
[23] N. Solodovchenko, K. Samusev, M. Limonov. Phys. Rev. B **109**, *7*, 075131 (2024).
[24] N. Solodovchenko, M. Bochkarev, K. Samusev, M. Limonov. Nanophoton. **14**, *18*, 3043 (2025).
[25] M. Bochkarev, N. Solodovchenko, G. Chekmarev, A. Ermina, K. Samusev, M. Limonov. Phys. Rev. B **112**, *8*, L081102 (2025).
[26] M. Bochkarev, N. Solodovchenko, K. Samusev, M. Limonov. Mater. Today **80**, 179 (2024).
[27] https://zetamix.fr/produit/filament-epsilon/. Access: Oct. 26, 2025.
[28] G.C. Righini, Y. Dumeige, P. F'eron, M. Ferrari, G. Nunzi Conti, D. Ristic, S. Soria. La Rivista del Nuovo Cimento **34**, *7*, 435 (2011).
[29] M.L.M. Balistreri, D.J.W. Klunder, F.C. Blom, A. Driessen, J.P. Korterik, L. Kuipers, N.F. van Hulst. J. Optical Soc. Am. B **18**, *4*, 465 (2001).
[30] D.A. Baranov, K.B. Samusev, I.I. Shishkin, A.K. Samusev, P.A. Belov, A.A. Bogdanov. Optics Lett. **41**, *4*, 749 (2016).
[31] M.F. Limonov, M.V. Rybin, A.N. Poddubny, Y.S. Kivshar. Nature Photon. **11**, *9*, 543 (2017).
[32] M.F. Limonov. Adv. Opt. Photon. **13**, *3*, 703 (2021).
[33] M.I. Tribelsky, A.E. Miroshnichenko. Phys. Rev. A **93**, *5*, 053837 (2016).

Translated by T.Zorina